Received April 28, 2021, accepted May 6, 2021, date of publication May 14, 2021, date of current version May 25, 2021.

Digital Object Identifier 10.1109/ACCESS.2021.3080575

Short-Term Hydrothermal Scheduling With Solar and Wind Farms Using Second-Order Cone Optimization With Chance-Box Constraints

JUAN CAMILO CASTAÑO[1], (Member, IEEE), ALEJANDRO GARCES[1], (Senior Member, IEEE), AND OLAV B. FOSSO[2], (Senior Member, IEEE)

[1]Department of Electric Power Engineering, Universidad Tecnológica de Pereira, Pereira 660003, Colombia
[2]Department of Electric Power Engineering, Norwegian University of Science and Technology, 7491 Trondheim, Norway

Corresponding author: Juan Camilo Castaño (lendonc@utp.edu.co)

ABSTRACT Short-Term Hydrothermal Scheduling (STHS) is a classic problem in power system operation where the aim is to decide the dispatch of both thermal and hydroelectric units. This problem is complex due to its non-linear non-convex nature, and the requirements for fast solving for daily operation. Technologies such as wind and solar generation introduce stochastic behaviors, which have to be considered within the mathematical model. Although the problem is frequently solved by traditional and heuristic techniques, this paper proposes a new formulation based on convex approximations, and in particular, Second-Order Cone optimization, which addresses the nonlinear relation among water discharge, reservoir volume, and hydropower generation in a rigorous mathematical approach. Moreover, the impact of wind and solar generation on the power system is analyzed, modeling their stochastic behavior in a robust way by using chance-box constraints. Numerical results demonstrate that the Second-Order Cone approximation is precise and faster than techniques proposed recently and that the chance-box constraint approach guarantees a robust solution.

INDEX TERMS Hydrothermal scheduling, economic dispatch, solar generation, wind generation, mathematical optimization, non-linear programming, chance-box constraints.

NOMENCLATURE

$(\cdot)^{\mathsf{g}}$	Type of generation unit with $\mathsf{g} \in \{\mathsf{h}, \mathsf{t}, \mathsf{w}, \mathsf{s}\}$ for hydro, thermal, wind, and solar, respectively
δ_{it}	Instance of random variable d_{it}
v_{cut-in}	Cut-in velocity of the wind turbine in m/s
$v_{cut-out}$	Cut-out velocity of the wind turbine in m/s
v_{it}	Wind velocity data for unit i at moment t in m/s
v_{nom}	Nominal velocity of the wind turbine in m/s
Ω_i	Set of nodes that are connected to node i for both the electrical and the hydraulic network
ϕ	Quantile function
ρ_{it}^{g}	Instance of random variable p_{it}^{g}
τ_i	Delay of hydroelectric unit i to immediate downstream plant
θ_{it}	Nodal angle at node i in time t
$\underline{x}, \overline{x}$	Minimum and maximum limits of variable x
ζ	Probability to comply a constraint
a_{it}	Inflow of hydroelectric unit i in time t
$c_{1i} - c_{6i}$	Coefficient of power generation function of hydro unit i
$c_{l_{1_i}} - c_{l_{3_i}}$	Coefficient of linearized power generation function of hydro unit i
cf_{it}	Capacity factor of generation unit i in time t
CU	Currency unit
d_t	Demand of the whole system in time t
d_{it}	Demand of node i in time t
e_{it}	Auxiliary variable
F	Cumulative distribution function
f_i	Cost function of thermal unit i
h_i	Output function of hydroelectric unit i
k_{it}	Auxiliary variable
n^{g}	Number of type g generation units
$O()$	Computational complexity function
p_{base}	Nominal power of the system in MW
$p_{i_{nom}}$	Nominal power of generation unit i

The associate editor coordinating the review of this manuscript and approving it for publication was R. K. Saket.

p^{f}_{ijt}	Power flow between nodes i and j in time t
p^{g}_{it}	Active power of generation unit i in time t in MW
pl^{h}_{i}	Hydropower of unit i using the linearized equation
pq^{h}_{i}	Hydropower of unit i using the quadratic equation
q_{it}	Flow of hydroelectric unit i in time t
r	Number of inputs of an algorithm
s_{it}	Spillage of hydroelectric unit i in time t
t	Time in hours
Tpl^{h}	Total hydropower by using the linearized equations
Tpq^{h}	Total hydropower by using the quadratic equations
u_{it}	Auxiliary variable
v_{it}	Water volume of reservoir i in time t

ACRONYMS

CPSO	Couple-Based Particle Swarm Optimization
CVX	Package for defining and solving convex problems
DE	Differential Evolution Algorithm
DRQEA	Differential Real-Coded Quantum-Inspired Evolutionary Algorithm
DWS/STHS-SOC	Deterministic Wind-Solar Short-Term Hydrothermal Scheduling using Second-Order Cone
HPDLQ	Difference between the total hydropower using linearized equations and the total hydropower using quadratic equations
inf	Infimum
Prob	Probability
PSO	Particle Swarm Optimization
QRSOS	Quasi-Reflected Symbiotic Organisms Search Algorithm
RWS/STHS-SOC	Robust Wind-Solar Short-Term Hydrothermal Scheduling using Second-Order Cone
SDP	Semi-definite Programming
SOC	Second-Order Cone
SOS	Symbiotic Organisms Search Algorithm
SPPSO	Small Population-Based Particle Swarm Optimization
STHS	Short-Term Hydrothermal Scheduling
STHS/SOC	Second-Order Cone Approximation for Short-Term Hydrothermal Scheduling

I. INTRODUCTION

A. MOTIVATION

Short-Term Hydrothermal Scheduling (STHS) is a non-linear optimization problem required in the operation of power systems including both hydroelectric and thermoelectric units. The problem is intrinsically non-convex and stochastic; moreover, modern power systems include wind and solar generation, which introduce new challenges. Therefore, it is necessary to develop approximations that deal effectively with the problem in this new context. Second-Order Cone optimization emerges as a suitable alternative to transform the problem into a convex model. Additionally, the stochastic behaviour of the problem can be considered as chance-box constraints generating a robust deterministic problem.

B. STATE OF THE ART

A large number of studies has been carried out concerning the STHS problem. Linear programming methods were considered in the early stage of the research [1], [2]. Mathematical decomposition has also been considered to determine the optimal scheduling [3]. At the beginning of the '90s, network flow programming was used to develop industrial applications for energy management systems. This approach implied a lower CPU time compared with other methodologies of this epoch [4], [5]. Additionally, the problem was studied under a Lagrangian relaxation approach in [6], [7]. Another conventional technique utilized to find a suitable solution was dynamic programming [8], [9]. This technique was widely used since results were provided at discrete load steps rather than at continuous load levels, which was satisfactory when the number of discrete states was not too large [10]. Furthermore, a four-dimensional piecewise linear model was proposed in [11], where spillage effects were considered, and the water head was taken into account as a function of forebay and tailrace levels. Mixed-integer linear programming formulations were also proposed for solving the problem in [12]–[15].

Nevertheless, these methods present some drawbacks. The size of the duality gap can affect the efficiency of Lagrangian relaxation; analysis of the gradient-based methods have shown that these methodologies tend to lead to local optimum points, and dynamic programming suffers from the curse of dimensionality. All of these methods use linearized models of an objective function and constraints, which may prevent the optimal solution of the problem from being obtained, due to the limitations of the linearization process [16].

Therefore, several authors have focused their studies on heuristic techniques. Among these techniques, genetic and evolutionary algorithms have been widely used owing to their flexibility, versatility, and ability to handle problems with complex inter-functional and intra-functional relationships, which each study presenting modifications of the crossover and mutation operators to improve the performance of the algorithms (see [17]–[20]). Nevertheless, these algorithms suffer from premature convergence, which leads to local optimums. To face this problem, particle swarm methodologies were proposed in [21]–[23]. Other approaches such as cuckoo search algorithms, clonal selection algorithm, and ant-lion optimization have shown several improvements in

the solution of the problem such as faster convergence and lower operation costs [24]–[26].

Despite their common use in power system applications, metaheuristic techniques have some limitations in terms of theory and practical implementations [27]. Therefore, a common approach dealing with non-linear problems is to generate convex approximations, which maintain the non-linear nature of the problem and guarantee global optimum and convergence of the algorithms. Convex approximations for the STHS problem is a relatively new subject. In [28] a semi-definite relaxation was proposed to face the combinatorial characteristic of the medium-term hydrothermal dispatch. In parallel, a semi-definite relaxation was presented in [29] to deal with the non-convexity of the hydropower equations in a rigorous mathematical way. However, semi-definite programming has to deal with a large number of sparse matrices, which implies a large computational burden.

Due to the renewable penetration in the system, the classic STHS problem needs to be modified to consider the special characteristics of these units. Thus, the impact of wind power was considered by deriving a closed form in terms of the incomplete gamma function in [30]. Otherwise, the uncertainty of wind and solar generation was taken into account in [31] under a scenario approach. Moreover, probabilistic Short-Term Hydrothermal Wind-Photovoltaic Scheduling based on the point estimate method was presented in [32].

A significant number of the investigations related to the STHS problem are based on heuristic algorithms. However, when it comes to the integration of renewable technologies, not only the technical aspects are important but also the economic element. By using a mixed-integer programming approach, [33] assessed important economic issues that arise with increased wind power penetration in hydrothermal systems. The results showed that restricting the injection of mandatory wind generation into the grid can reduce the total operation cost. This type of analysis requires concepts such as dual variables, which are not directly available in metaheuristic algorithms. Therefore, more formal techniques are required to make economic assessments after solving the optimization problem.

The STHS is closely related to the unit commitment (UC) problem, which pursues establishing the on/off status of the units for each period. Thus, several approaches have been proposed to deal with the UC problem. On one hand, mixed-integer linear programming has been used in [34]–[36] where linearized models are utilized. On the other hand, heuristic and metaheuristic techniques have also been implemented in [37]–[39]. Moreover, Lagrangian relaxations and Bender's decomposition approaches have been proposed in [40] and [41], respectively. The stochastic nature of wind generation has been considered in this problem too. In doing so, a chance-constrained two-stage programming approach is developed in [42] to address the unit commitment problem where compressed air energy storage, wind generation, and demand response programs are considered. The UC problem can be executed together with the STHS problem although both problems have their own mathematical complexity. Combined approaches of these two problems are usually formulated in terms of mixed-integer linear programming models that neglect the non-linear characteristics of hydraulic units.

It is worth mentioning that other aspects like the topology, time delays, and tailrace can make this problem more complicated. Thus, in [43] a junction network method to model complex tunnel networks in Short-Term Hydropower Scheduling is presented. Otherwise, water delays can be represented as multiples of the time resolution, an integer variable, a real number constant or a continuous variable [44]. Moreover, head loss due to the tailrace effect (an accumulation of water downstream of the hydro plant) varies considerably in the short term, and it is often represented by a polynomial of the fourth degree. This issue has been recently faced in [45], [46]. To better illustrate the proposed methodology, topology issues and tailrace variation are not considered. In addition, water delays are represented as a real number constant.

C. CONTRIBUTION

The contributions of this paper are twofold. Firstly, a Second-Order Cone (SOC) approximation is proposed based on modern convex optimization. To the authors' knowledge, there are few convex approximations for the problem, with the exception of the semi-definite approximations proposed in [29]. That approximation did not consider renewable energies but demonstrated that it is possible to obtain convex approximations without resorting to linearizations and heuristics. The Second-Order Cone approximation proposed here is more efficient and scalable, with high accuracy. Secondly, load, wind, and solar energies were included in the model via chance-box constraints. This approach allows us to consider the stochastic nature of the problem in a robust framework. In addition, the model presented here includes the transmission grid by a DC power flow.

D. OUTLINE

The rest of the paper is organized as follows: Section 2 presents the traditional non-linear non-convex STHTS model and its Second-Order Cone approximation; Section 3 presents the procedure for including the grid and the renewable sources in this problem; In Section 4, a methodology to deal with the stochastic aspects of the load and renewable sources is developed; Section 5 shows the results obtained for the proposed models; results are summarized in Section 6; conclusions are presented in Section 7; Appendix A presents the equivalence between a quadratic inequality constraint and a Second-Order Cone constraint; and Appendix B shows results given by a common linearization and some

of the drawbacks of working with it. Finally, references are presented.

II. SHORT-TERM HYDROTHERMAL SCHEDULING

To illustrate how to deal with the non-convexity of the problem, let us explain the traditional STHS model and the convex relaxation carried out.

A. BASIC STHS MODEL

The basic model for the STHS is presented in (1)

$$\begin{aligned}
\min \ & \sum_{i=1}^{n^{\mathsf{t}}} f_i(p_{it}^{\mathsf{t}}) \\
& p_{it}^{\mathsf{h}} = h_i(v_{it}, q_{it}) \\
& v_{it} = v_{it-1} + a_{it} - q_{it} - s_{it} + \sum_{j \in \Omega_i} q_{jt-\tau_i} + s_{jt-\tau_i} \\
& \sum_{i=1}^{n^{\mathsf{t}}} p_{it}^{\mathsf{t}} + \sum_{i=1}^{n^{\mathsf{h}}} p_{it}^{\mathsf{h}} = d_t \\
& \underline{v}_i \le v_{it} \le \overline{v}_i \\
& \underline{q}_i \le q_{it} \le \overline{q}_i \\
& \underline{p}_i^{\mathsf{g}} \le p_{it}^{\mathsf{g}} \le \overline{p}_i^{\mathsf{g}} \\
& 0 \le s_{it} \le \overline{s}_i \\
& v_{i1} = v_i^{\text{initial}} \\
& v_{i24} = v_i^{\text{end}}
\end{aligned} \tag{1}$$

The objective function consists of a sum of functions f_i, which represents either cost or CO_2 emission. These functions are usually quadratic and convex. Each hydroelectric power plant is represented by a non-linear function h_i given by (2) [20], [29].

$$\begin{aligned}
p_{it}^{\mathsf{h}} = h(v_{it}, q_{it}) = & -c_{1i}v_{it}^2 - c_{2i}q_{it}^2 \\
& + c_{3i}v_{it}q_{it} + c_{4i}v_{it} + c_{5i}q_{it} + c_{6i}
\end{aligned} \tag{2}$$

where $[c_{1i}, \ldots, c_{6i}]$ are known constants for each hydroelectric unit i. This equation is clearly non-convex and shows the complexity of the problem. Figure 1 depicts this function for a particular hydroelectric unit.

The model deals with hydraulic chains like the one shown in Figure 2. This hydro-reservoir network considers natural inflows of each unit a_{it}, spillage s_{it}, and actual flow that generates power q_{it}. The volume in the reservoir is consequently modified by these flows. Note that the flow that comes from an upper reservoir to a lower reservoir does not arrive immediately; therefore, a time delay τ_i must be considered in each branch of the hydraulic network.

The other constraints of Model (1) are the balance of power, box constraints of the variables, and initial/final conditions of the reservoir.

B. SECOND-ORDER CONE APPROXIMATION

Note that most of the constraints in Model (1) are convex. However, (2) is a non-affine equality equation. Recent investigations ([28] and [29]) have proposed semi-definite

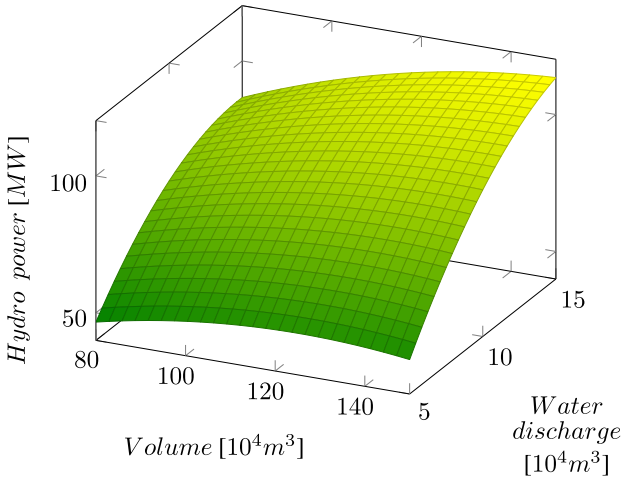

FIGURE 1. Quadratic function for a hydro-power unit with $c_1 = 0.0042$, $c_2 = 0.42$, $c_3 = 0.03$, $c_4 = 0.9$, $c_5 = 10$ and $c_6 = -50$.

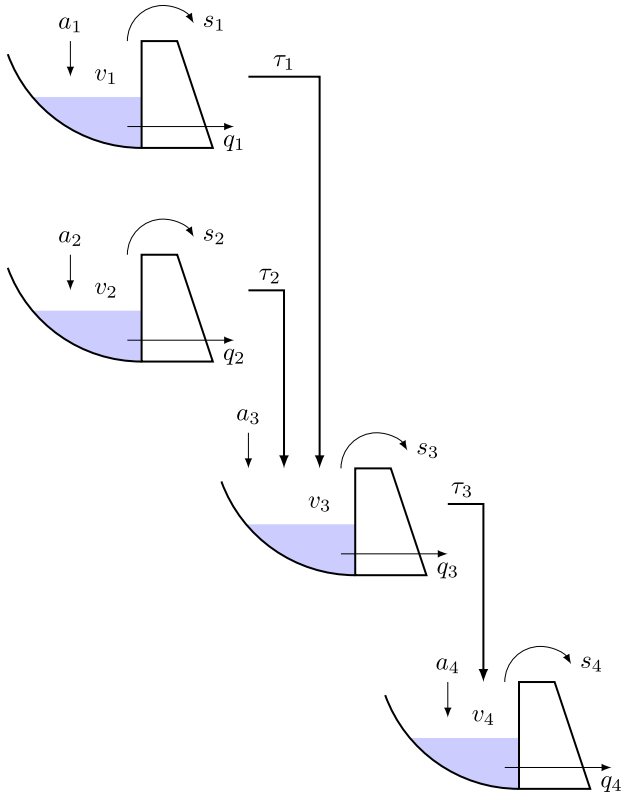

FIGURE 2. Example of a hydraulic chain. a_i represents inflows, v_i volume, q_i flow, s_i spillage, and τ_i delays.

approximations for these constraints. This approach transforms the non-convex constraints into a matrix-space with convex geometry. Although this type of transformation improves the geometric properties of the problem, it increases the feasible region from $\mathbb{R}^n$ to $\mathbb{R}^{n \times n}$. Therefore, the problem can be computationally expensive.

On the other hand, Second-Order Cone optimization is a convex programming alternative that has been widely used in several electrical engineering problems such as designing even-order finite-impulse-response variable fractional-delay

digital filters [47], developing new control strategies [48] and AC-DC power flow [49]. SOC requires less computational effort than semi-definite programming. To the best of the authors' knowledge, SOC programming has not been used to solve the STHS problem.

A Second-Order Cone is a convex space represented by (3).

$$\|x\| \leq z \tag{3}$$

where $x \in \mathbb{R}^n$ and $z \in \mathbb{R}$. $\|x\|$ is the norm-2 of the vector x (hence it is also called a Euclidean cone). Figure 3 shows a Second-Order Cone in $\mathbb{R}^3$ with components x_1, x_2 and z. This is clearly a convex cone.

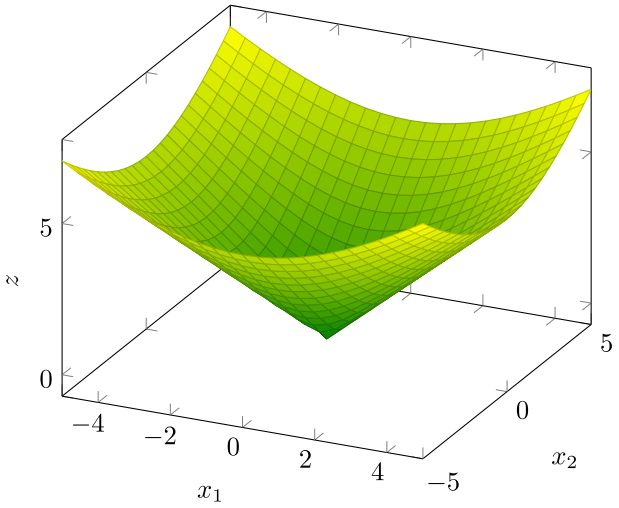

FIGURE 3. Representation of the second-order cone $\Omega = \{\|x\| \leq z\}$ with $x \in \mathbb{R}^2$ and $z \in \mathbb{R}$.

Moreover, SOC algorithms are well-known for their low computational complexity of $\sqrt{r}$ for problems with r Second-Order Cone inequalities [50], which is essential to escalate said algorithm in problems with a large number of inputs.

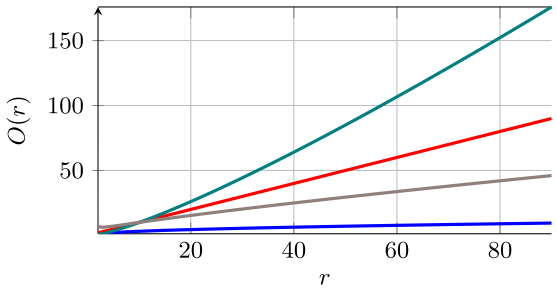

FIGURE 4. $\sqrt{r}$ (——), $r\log(r)$ (——), $r/\log(r)$ —— and r (——) computational complexity functions.

Figure 4 depicts how the computational complexity increases as the inputs increase. In computational science, algorithms that run in linear or r-log-r times are considered algorithms with a suitable scalability [51]. From the aforementioned figure, it can be observed that SOC has a computational complexity that is lower than linear and r-log-r times, which proves its robustness when it comes to increasing the number of inputs of the problem.

To obtain a SOC approximation of (2), a matrix representation of the quadratic form h is proposed as given in (4).

$$h(x) = -x^\top Ax + b^\top x + c_{6i} \tag{4}$$

with $x = (v_{it}, q_{it})^\top$, A is a matrix given by (5) and b is a vector given by (6).

$$A = \begin{pmatrix} c_{1i} & -\frac{1}{2}c_{3i} \\ -\frac{1}{2}c_{3i} & c_{2i} \end{pmatrix} \tag{5}$$

$$b = (c_{4i}, c_{5i})^\top \tag{6}$$

Note that $A \succeq 0$ (i.e., is positive semi-definite) if $c_{1i} \geq 0$ and $c_{1i}c_{2i} - \frac{1}{4}c_{3i}^2 \geq 0$. In that case, A has Cholesky factorization $A^{\frac{1}{2}}$ given by (7).

$$A^{\frac{1}{2}} = \begin{pmatrix} \sqrt{c_{1i}} & -\frac{c_{3i}}{2\sqrt{c_{1i}}} \\ 0 & \sqrt{c_{2i} - \frac{c_{3i}^2}{4c_{1i}}} \end{pmatrix} \tag{7}$$

The approximation of (2) is obtained by transforming the equality into an inequality constraint using the matrix representation (4) as follows:

$$p_{it}^{\mathsf{h}} + x^\top Ax - b^\top x - c_{6i} \leq 0 \tag{8}$$

which can be transformed into a SOC constraints as given in (9).

$$\left\| \begin{pmatrix} A^{\frac{1}{2}}x \\ \frac{1 - b^\top x - c_{6i} + p_{it}^{\mathsf{h}}}{2} \end{pmatrix} \right\| \leq \frac{1 + b^\top x + c_{6i} - p_{it}^{\mathsf{h}}}{2} \tag{9}$$

This constraint is convex and can be solved efficiently using interior point methods [50] (further information is provided in [52]). It is important to highlight that the approximation remains in $\mathbb{R}^3$ in contrast to semi-definite approximations that transform the problem into a space $\mathbb{R}^{3\times3}$. Therefore, SOC problems can be solved more efficiently than semi-definite programming. The SOC approximation of (1) consists of replacing (9) in the constraint that includes h. This model will be referred as STHS-SOC for the rest of the paper. Appendix A explains the equivalence between (8) and (9).

III. INCORPORATING THE GRID AND RENEWABLE GENERATION

The traditional STHS problem must be modified to consider renewable generation units, which are more common nowadays, and the constraints that the grid imposes. Therefore, it is necessary to model the power produced by wind and solar units and include the effects of the grid.

A. WIND AND SOLAR GENERATION

The power produced by photovoltaic solar units depends on several factors: poor orientation and inclination of the solar panels imply a reduction of the generated power; the latitude of the place where they are installed is a key factor when

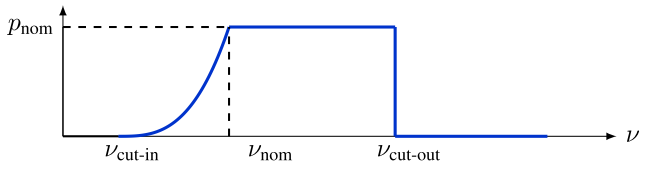

FIGURE 5. Output power as a function of the wind speed for typical control.

establishing the amount of available resources; cloudiness is another factor that impacts considerably on the availability of these generation units; and high temperatures reduce the efficiency of the energy conversation carried out in these devices. In doing so, all of these elements that constrain the solar power produced must be taken into account with regard to analyzing their operation. However, the concept of power capacity allows us to calculate the generated power as a function of its power capacity and nominal power. By doing so, the output power of a unit i at the time instant t is given by (10). Note that the power irradiation is zero at hours without sun and reaches its peak around noon.

$$p^{\mathsf{s}}_{it} = cf^{\mathsf{s}}_{it} \cdot p^{\mathsf{s}}_{i_{nom}} \tag{10}$$

On the other hand, the output power of a wind turbine presents a discontinuous characteristic due to its type of control. For wind velocities below $\nu_{\text{cut-in}}$, the output power is zero; from $\nu_{\text{cut-in}} \leq \nu \leq \nu_{\text{nom}}$ the turbine is controlled for maximum power tracking, therefore, the output power depicts a cubic function; from $\nu_{\text{nom}} \leq \nu \leq \nu_{\text{cut-out}}$, the pitch angle control maintains constant power; finally, for $\nu \geq \nu_{\text{cut-out}}$ the turbine is mechanically blocked to protect the internal devices. Figure 5 shows the output power as a function of the wind speed for a wind turbine, while (11) is its corresponding equation.

$$p^{\mathsf{w}}_{it} = \begin{cases} 0 & \nu_{it} \leq \nu_{\text{cut-in}} \\ p^{\mathsf{w}}_{i_{\text{nom}}} \left(\dfrac{\nu_{it} - \nu_{\text{cut-in}}}{\nu_{\text{nom}} - \nu_{\text{cut-in}}}\right)^3 & \nu_{\text{cut-in}} \leq \nu_{it} \leq \nu_{\text{nom}} \\ p^{\mathsf{w}}_{i_{\text{nom}}} & \nu_{\text{nom}} \leq \nu_{it} \leq \nu_{\text{cut-out}} \\ 0 & \nu_{it} \geq \nu_{\text{cut-out}} \end{cases} \tag{11}$$

B. INCLUDING THE GRID AND WIND/SOLAR GENERATION

The STHS-SOC model is modified to include grid constraints as well as wind and solar generation. The grid is represented by a linear model with power flows p^{f}_{ijt} and angles θ_{it}, while the renewable generation units are modeled by (10) and (11).

For the sake of completeness, the model is presented below.

$$\min \sum_{i=1}^{n^{\mathsf{t}}} f_i(p^{\mathsf{t}}_{it})$$

$$\left\| \begin{pmatrix} \sqrt{c_{1i}}\, v_{it} - \dfrac{c_{3i} q_{it}}{2\sqrt{c_{1i}}} \\ \sqrt{c_{2i} - \dfrac{c^2_{3i}}{4c_{1i}}}\, q_{it} \\ \frac{1}{2}(1 - u_{it}) \end{pmatrix} \right\| \leq \frac{1 + u_{it}}{2}$$

$$u_{it} = c_{4i} v_{it} + c_{5i} q_{it} + c_{6i} - p^{\mathsf{h}}_{it}$$

$$v_{it} = v_{it-1} + a_{it} - q_{it} - s_{it} + \sum_{j \in \Omega_i} q_{jt-\tau_i} + s_{jt-\tau_i}$$

$$p^{\mathsf{g}}_{it} - d_{it} = \sum_{j \in \Omega_i} p^{\mathsf{f}}_{ijt}$$

$$p^{\mathsf{f}}_{ijt} = p_{\text{base}} \frac{\theta_{it} - \theta_{jt}}{x_{ij}}$$

$$\underline{v}_i \leq v_{it} \leq \overline{v}_i$$

$$\underline{q}_i \leq q_{it} \leq \overline{q}_i$$

$$\underline{p}^{\mathsf{g}}_i \leq p^{\mathsf{g}}_{it} \leq \overline{p}^{\mathsf{g}}_i$$

$$0 \leq s_{it} \leq \overline{s}_i$$

$$-\overline{p}^{\mathsf{f}}_{ij} \leq p_{ijt} \leq \overline{p}^{\mathsf{f}}_{ij}$$

$$-\overline{\theta}_i \leq \theta_{it} \leq \overline{\theta}_i$$

$$\theta_{1t} = 0$$

$$v_{i1} = v^{\text{initial}}_i$$

$$v_{i24} = v^{\text{end}}_i$$

$$p^{\mathsf{g}}_{it} = cf^{\mathsf{g}}_{it} \cdot p^{\mathsf{g}}_{i_{nom}}, \text{ for } \mathsf{g} \in \{\mathsf{s}\}$$

$$p^{\mathsf{g}}_{it} = \begin{cases} 0 & \nu_{it} \leq \nu_{\text{cut-in}} \\ p^{\mathsf{w}}_{i_{\text{nom}}} \left(\dfrac{\nu_{it} - \nu_{\text{cut-in}}}{\nu_{\text{nom}} - \nu_{\text{cut-in}}}\right)^3 & \nu_{\text{cut-in}} \leq \nu_{it} \leq \nu_{\text{nom}} \\ p^{\mathsf{w}}_{i_{\text{nom}}} & \nu_{\text{nom}} \leq \nu_{it} \leq \nu_{\text{cut-out}} \\ 0 & \nu_{it} \geq \nu_{\text{cut-out}} \end{cases} \tag{12}$$

where u_{it} is an auxiliary variable. Note that this model is deterministic and does not consider the stochasticity of renewable sources. Consequently, it will be called DWS/STHS-SOC from now on.

IV. CONSIDERING THE STOCHASTICITY OF THE RANDOM VARIABLES

The stochastic nature of the load, wind, and solar generation is represented by probability constraints with a given probability ζ as follows:

$$\text{Prob}\left(p^{\mathsf{g}}_{it} \geq \rho^{\mathsf{g}}_{it}\right) \geq \zeta, \text{ for } \mathsf{g} \in \{\mathsf{w}, \mathsf{s}\} \tag{13}$$

$$\text{Prob}\left(d_{it} \leq \delta_{it}\right) \geq \zeta \tag{14}$$

In this way, the model that considers the stochastic behavior of the load, wind, and solar generation is given by (15) in which wind and solar power equations are replaced by (13), and (14) is included to consider the stochastic nature of the load.

$$\min \sum_{i=1}^{n^{\mathsf{t}}} f_i(p^{\mathsf{t}}_{it})$$

$$\left\| \begin{pmatrix} \sqrt{c_{1i}}\, v_{it} - \dfrac{c_{3i} q_{it}}{2\sqrt{c_{1i}}} \\ \sqrt{c_{2i} - \dfrac{c^2_{3i}}{4c_{1i}}}\, q_{it} \\ \frac{1}{2}(1 - u_{it}) \end{pmatrix} \right\| \leq \frac{1 + u_{it}}{2}$$

$$
\begin{aligned}
& u_{it} = c_{4i} v_{it} + c_{5i} q_{it} + c_{6i} - p^{\mathsf{h}}_{it} \\
& v_{it} = v_{it-1} + a_{it} - q_{it} - s_{it} + \sum_{j \in \Omega_i} q_{jt-\tau_i} + s_{jt-\tau_i} \\
& p^{\mathsf{g}}_{it} - d_{it} = \sum_{j \in \Omega_i} p^{\mathsf{f}}_{ijt} \\
& p^{\mathsf{f}}_{ijt} = p_{\text{base}} \frac{\theta_{it} - \theta_{jt}}{x_{ij}} \\
& \underline{v}_i \le v_{it} \le \overline{v}_i \\
& \underline{q}_i \le q_{it} \le \overline{q}_i \\
& \underline{p}^{\mathsf{g}}_i \le p^{\mathsf{g}}_{it} \le \overline{p}^{\mathsf{g}}_i \\
& 0 \le s_{it} \le \overline{s}_i \\
& -\overline{p}^{\mathsf{f}}_{ij} \le p_{ijt} \le \overline{p}^{\mathsf{f}}_{ij} \\
& -\overline{\theta}_i \le \theta_{it} \le \overline{\theta}_i \\
& \theta_{1t} = 0 \\
& v_{i1} = v^{\text{initial}}_i \\
& v_{i24} = v^{\text{end}}_i \\
& \text{Prob}\left(p^{\mathsf{g}}_{it} \ge \rho^{\mathsf{g}}_{it}\right) \ge \zeta, \ \text{for} \ \mathsf{g} \in \{\mathsf{w}, \mathsf{s}\} \\
& \text{Prob}\left(d_{it} \le \delta_{it}\right) \ge \zeta
\end{aligned} \tag{15}
$$

The probabilistic constraints are transformed into deterministic counterparts using a robust approach. Both the wind velocity and the solar radiation are adjusted to Weibull distributions. Figure 6 shows a density function and a cumulative function for wind speeds with Weibull distribution. The output power for a solar-photovoltaic system is proportional to the radiation and therefore, the distribution of p^{s} is also expected to be Weibull. However, the output power of a wind turbine presents a discontinuous characteristic due to its type of control as Figure 5 depicts.

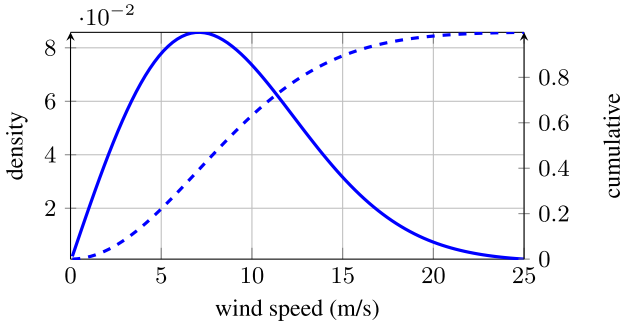

FIGURE 6. Density function (——) and cumulative function (- - -) for the Weibull distribution.

Consequently, the output power p^{w} presents a distribution that is not smooth and needs to be evaluated numerically; its density function presents dirac-type discontinuities in $p^{\mathsf{w}} = 0$ and $p^{\mathsf{w}} = p_{\text{nom}}$ whereas it is continuous between 0 and p_{nom}.

Provided the cumulative distribution of the power $F(\rho)$, the probability of a specific output power is given by (16).

$$F(\rho) = \text{Prob}\,(p \ge \rho) \tag{16}$$

A quantile function associated with the probability distribution of the generated power is defined as (17) [53].

$$\phi(\zeta) = \inf\{\rho \in \mathbb{R} : \zeta \le F(\rho)\} \tag{17}$$

Therefore, it is possible to define an upper bound for the generated power given a probability ζ as given in (18).

$$\overline{p}^{\mathsf{g}}_{it} = \phi_\rho(1 - \zeta) \ \text{for} \ \mathsf{g} \in \{\mathsf{w}, \mathsf{s}\} \tag{18}$$

This upper bound is included directly into the optimization model as a constraint of the form of (19) [54].

$$0 \le p^{\mathsf{g}}_{it} \le \overline{p}^{\mathsf{g}}_{it}, \ \text{for} \ \mathsf{g} \in \{\mathsf{w}, \mathsf{s}\} \tag{19}$$

This constraint is guaranteed with a probability ζ, thus, ζ is a measure of robustness for the problem. The same procedure is applied to the power demand, obtaining a lower bound $\underline{d}_{it}$ as follows.

$$\underline{d}_{it} = \phi_\delta(\zeta) \tag{20}$$

This lower bound is included in the model as a deterministic constraint as given below:

$$d_{it} \ge \underline{d}_{it} \tag{21}$$

The power demand is represented by a uniform distribution.

The model with the Second-Order Cone approximation, the grid, and the chance-box constraints for the load, wind, and solar generators will be called RWS/STHS-SOC from this point forward.

V. RESULTS

Four sets of simulations were carried out to test the proposed models and compare them. First, it was only considered a hydrothermal model (STHS-SOC model) for the purpose of comparing the obtained results with previous studies that had used the same test system (see [20]). In this model, the spillage was considered equal to zero as in the previous research.

Then, a convex-deterministic Short-Term Hydrothermal-Wind Solar model was tested without considering the stochastic nature of the renewable resources and load (DWS/STHS-SOC model). For this simulation, the values of wind speed and solar capacity were considered as the mean value of the data per hour.

Next, a stochastic model was implemented by considering a robust set of 80% to comply the chances constraint of this model (RWS/STHS-SOC, case I). After that, the same model was tested but, in this case, the probability to comply the chance constraints was considered 60% (RWS/STHS-SOC, case II). Note that a probability of 100% would be an extremely robust approach that would lead to pessimistic solutions of the problem since the equivalent values, for wind and solar generation, would be zero (see (18), and Figures 17 and 18). On the other hand, probabilities under 50% would not be of interest since they are not going to be robust enough. Therefore, it makes sense to assume probabilities of 60% and 80% to illustrate the proposed methodology.

TABLE 1. Characteristics of wind farm.

$p_{\text{nom}}[MW]$	$\nu_{\text{cut-in}}\ [m/s]$	$\nu_{\text{nom}}\ [m/s]$	$\nu_{\text{cut-out}}\ [m/s]$
2	4	12	25

Nevertheless, this is a parameter that is going to depend on the requirements of the system operator.

Finally, it is important to highlight that for the DWS/STHS-SOC and RWS/STHS-SOC models, the upper limits of spillage were considered equal to $2 \times 10^4 \frac{m^3}{h}$ to study how these variables affect the optimization process [29]. All models were solved in a 3.2GHz Intel Core i8-8700 PC with 8 GB RAM using CVX in MATLAB, a package for defining and solving convex problems.

A. TEST SYSTEM

The test system used to evaluate the performance of the DWS/STHS-SOC and RWS/STHS-SOC models consists of a multi-chain cascade of 4 hydro units, a number of thermal units represented by an equivalent thermal plant, a photovoltaic solar farm, and a wind farm. Additionally, the new England IEEE-39 bus system was considered. The location of the generators and the distribution of load are presented in Figure 7. Moreover, the power limits of the lines were considered as the inverse of the reactance per unit divided 6.5. This assumption was based on the maximum angle stability and its relation to the maximum temperature capability [55], [56].

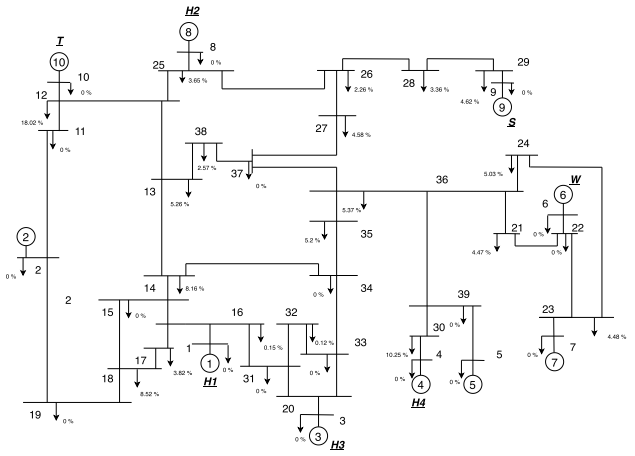

FIGURE 7. New England, IEEE 39 bus-system.

The wind farm considered in this test system consists of 340 wind turbines. Their characteristics are presented in Table 1. On the other hand, the solar farm consists of 2,500,000 photovoltaic panels, each with a nominal power equal to 240 watts, which adds a nominal power for the solar farm equal to 600 megawatts.

The quantile function of solar power was built with capacity factor data taken from [57]. These data pertain to the recorded hourly data for every month of June between 1979 and 2017 in Spain. Said data correspond to units with solar trackers.

Wind speed data used to build the quantile function of wind power were taken from the wind prospector of The National Renewable Energy Laboratory of The United States. These data belong to the recorded hourly data for June in Hawaii.

In addition, the characteristics of the hydro-chain, thermal power plant, and load were taken from [20]. It is worth mentioning that the values of coefficients C_1 and C_2 considered in our research are equivalent to the values of $-C_1$ and $-C_2$ considered in [20] as Table 2 shows. Nevertheless, the hydropower equations of the form of (2) remain the same due to the structure that we chose to represent them. The data of the considered grid were taken from [58].

TABLE 2. Hydropower coefficients.

Plant	C_1	C_2	C_3	C_4	C_5	C_6
1	-0.0042	-0.42	0.030	0.90	10	-50
2	-0.0040	-0.30	0.015	1.14	9.5	-70
3	-0.0016	-0.30	0.014	0.55	5.5	-40
4	-0.0030	-0.31	0.027	1.44	14	-90

To sum up, the total installed power of the system is 5,780 MW, where the hydro generation adds 43.3 % of the total capacity (4 hydro units of 500 MW); 34.61 % is thermal (an equivalent thermal plant of 2,500 MW); 11.76 % is wind (340 wind turbines of 2 MW) and 10.38 % is solar (2,500,000 photovoltaic panels of 240 watts).

B. STHS-SOC

To have a framework to compare the time convergence and accuracy of the proposed methodology, STHS-SOC is tested by using the system presented in [20]. Table 3 shows a comparison of results obtained for several methodologies implemented in the mentioned test system. For the sake of simplicity, only time convergence and the value of the objective function are compared.

TABLE 3. Optimal cost and CPU time of SOC and other methodologies.

Methodology	Objective function[CU]	CPU time [s]
STHS-SOC	925866.00	4.7
SDP I [29]	925866.00	———
CPSO [22]	922328.64	18.6
SPPSO [21]	922336.31	16.3
DE [19]	923234.56	8.69
DRQEA [19]	922526.73	7.98
SOS [59]	922338.20	6.21
QRSOS [59]	922329.94	5.16

It is clear that SOC presents a superior performance regarding time convergence compared with other techniques proposed in the past. Additionally, its computational complexity of $\sqrt{r}$ presents a considerable computational advantage compared with the most popular heuristic techniques, which report computational complexity of r, $rlog(r)$, and $r/log(r)$ [60]–[62]. Nevertheless, it is worth being careful when it comes to comparing CPU times since they can be

affected by the computing power where the simulations were carried out.

Another interesting result from Table 3 is that SOC and semi-definite programming find the same optimum, which is one of the fundamental attributes of convex optimization. This is a remarkable distinction contrasted with metaheuristic techniques.

It is noteworthy that the results of metaheuristic techniques presented in Table 3 only give us an idea about the possible solution to the problem; these techniques do not guarantee a global optimum since their operation is stochastic by nature. The exact solution to non-convex optimization problems is still an open problem. Therefore, there is no way to carry out an exact comparison regarding the value of the objective function.

C. DWS/STHS-SOC

The obtained results, for all simulations carried out, show the same behavior for hydropower plants. This is explained by considering the zero costs of the power produced by these units. Consequently, the optimization algorithm schedules the units with zero operation costs first, and then dispatches the thermal units. Thus, when different renewable generation and load values are considered, the hydropower is scheduled in the same optimal way, while the thermal power is modified regarding the values of load, wind generation, and solar generation.

For the sake of simplicity, only the behavior of hydro units is analyzed for this model. However, as was mentioned before, this behavior is the same for all sets of simulations.

Note that the previous analysis is only valid for hydro units without a pumping system. If units have any kind of storage system, without associated cost, they will take some of the variation of the renewable units to avoid drastic variation of the thermal power production.

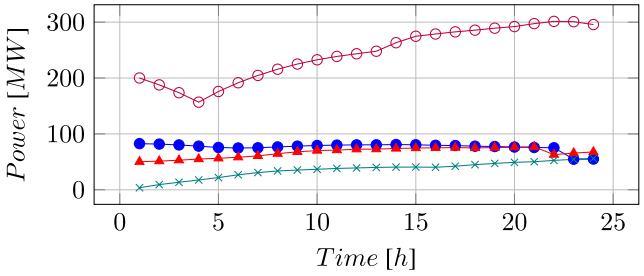

FIGURE 8. Power produced by hydro units (all models) (—●—) Unit 1, (—▲—) Unit 2, (—×—) Unit 3, (—○—) Unit 4.

From Figures 8, 9 and 10, it can be observed that the amount of power produced by unit 3 tends to be low in some intervals, even though the volume and the water discharge are not low, which seems to contradict (2), where the hydropower is proportional to the water discharges and the volume of the reservoirs. Nevertheless, this behavior makes sense if we consider that the coefficients c_i of unit 3 are the smallest value

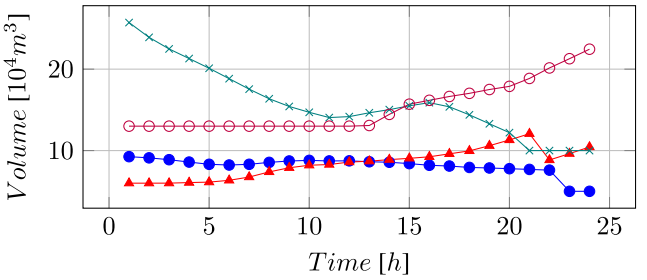

FIGURE 9. Water discharge of hydro units (all models) (—●—) Unit 1, (—▲—) Unit 2, (—×—) Unit 3, (—○—) Unit 4.

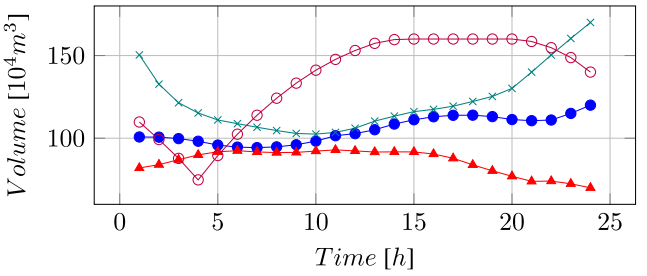

FIGURE 10. Volumes of reservoirs (all models) (—●—) Res 1, (—▲—) Res 2, (—×—) Res 3, (—○—) Res 4.

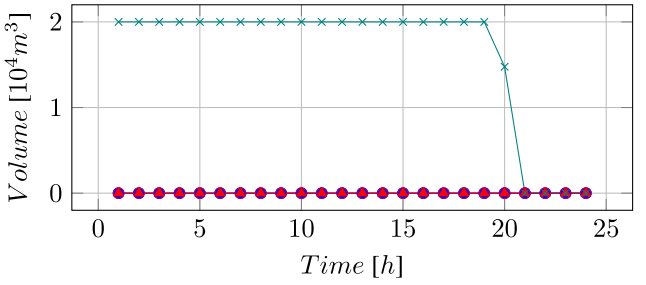

FIGURE 11. Spillage (all models) (—●—) Res 1, (—▲—) Res 2, (—×—) Res 3, (—○—) Res 4.

compared with the others (see [20]). This means that unit 3 is the least efficient of the hydro-chain.

In addition, Figures 8, 9, 10, and 11 show that the optimization model tends to reduce the volume of reservoir 3 (without violating the final values of the volume) while the volume of reservoir 4 increases. The reason for this is that unit 4 is more capable of producing power than unit 3 (an interested reader can evaluate (2) with the coefficients of unit 3 and unit 4 and will note that, for the same values of volume and water discharges, the produced power by unit 4 will be larger than the produced power of unit 3). That is why the model tends to produce power by using unit 4 rather than unit 3. Thus, the spillage of reservoir 3 tends to be as large as possible until the volume of reservoir 4 needs to decrease to reach the final value. Further, analyzing the dual variables of the upper bound of spillage can be useful to understand this behavior better. Figure 12 depicts the rate of change of the objective function with respect to the upper bound of the spillage. Note that this dual variable for reservoir 3 impacts

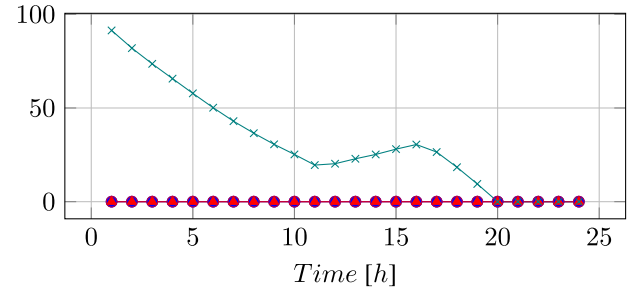

FIGURE 12. Dual variable of spillage (all models) (—●—) Res 1, (—▲—) Res 2, (—×—) Res 3, (—○—) Res 4.

the objective function considerably while the dual variables of reservoir 1, 2, and 4 do not. This implies that allowing spillage to be different from zero, can decrease the operation cost of the power system. It is important to highlight that this kind of analysis cannot be carried out when heuristic and metaheuristic techniques are used.

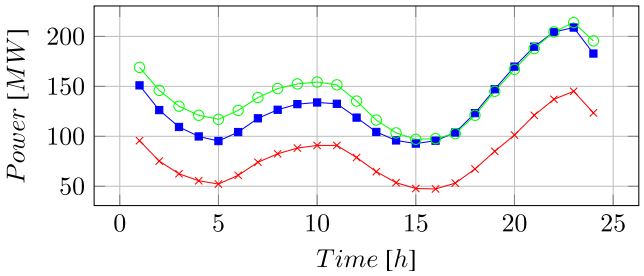

FIGURE 13. Power produced by wind unit (models with renewable energy) (—■—) Deterministic, (—×—) $\zeta = 80\%$, (—○—) $\zeta = 60\%$.

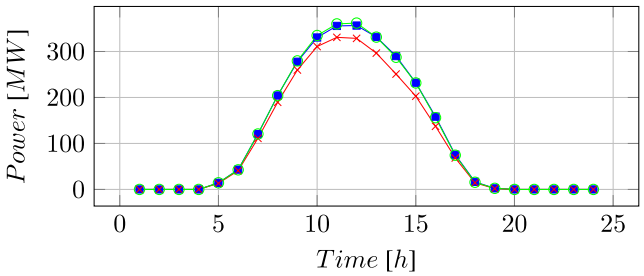

FIGURE 14. Power produced by solar (models with renewable energy) (—■—) Deterministic, (—×—) $\zeta = 80\%$, (—○—) $\zeta = 60\%$.

On the other hand, Figure 13 shows wind power behavior, which reaches its peaks of power production in the intervals of time between 10-12 hours and between 22-24 hours. This behavior is due to the particular characteristics of the wind resource in the place where the data were measured. In another way, Figure 14 shows that the peak of solar generation is between 10 and 13 hours. This shaves the peak of thermal power produced between this interval of time. Moreover, the solar production continues until 18 hours. This means that the production of thermal power has to increase quickly to supply the maximum power consumption at 20 hours (see Figures 15 and 16). Note that this analysis is valid for all

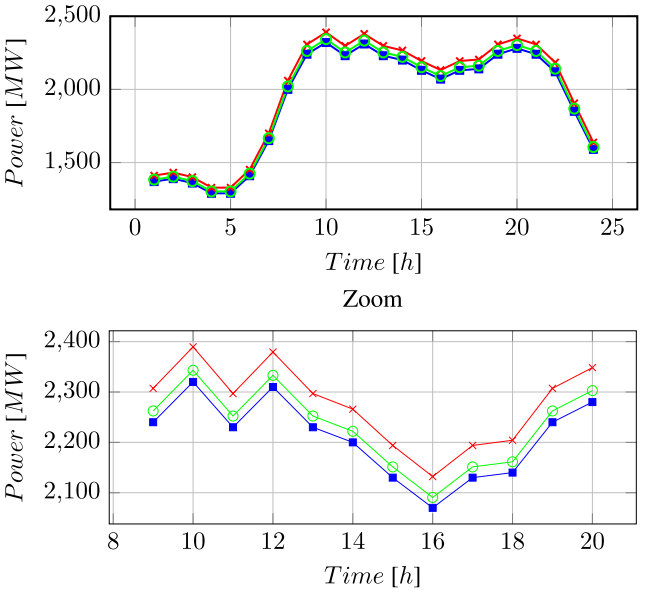

FIGURE 15. Power consumed (models with renewable energy) (—■—) Deterministic, (—×—) $\zeta = 80\%$, (—○—) $\zeta = 60\%$.

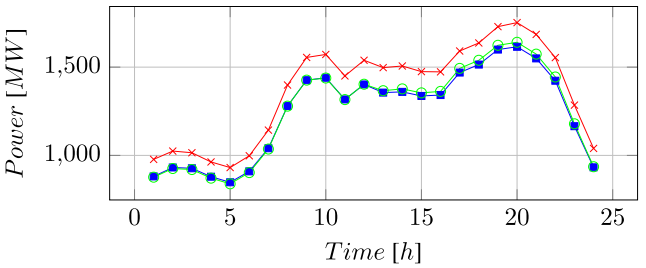

FIGURE 16. Power produced by thermal unit (models with renewable energy) (—■—) Deterministic, (—×—) $\zeta = 80\%$, (—○—) $\zeta = 60\%$.

models studied; the only difference is the magnitude of the aforementioned variables.

D. RWS/STHS-SOC MODEL

This model was used to evaluate two cases. First, the ζ values were set in 80% (RWS/STHS-SOC model, case I). Then, they were set in 60% (RWS/STHS-SOC model, case II) to see how the results change when these parameters change. For the sake of simplicity, the values of the quantile function were calculated by using MATLAB's *quantile* function.

In both cases, the behavior of hydro generation is the same compared with DWS/STHS-SOC. The reason why it does not change is that considering the stochasticity of the load, wind, and solar generation in the optimization model will affect the thermal power production, which is the only variable that directly affects the value of the objective function since the water costs are considered zero. Thus, the water discharges (Figure 9) volume of reservoirs (Figure 10), spillage (Figure 11) and dual variable of the upper limit of spillage (Figure 12) remain the same.

On the other hand, wind generation (Figure 13), solar generation (Figure 14), and load demand (Figure 15) are modified when the stochasticity of these random variables

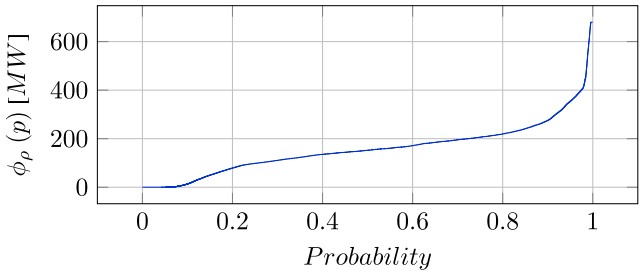

FIGURE 17. Quantile function of wind power at 12 pm (——).

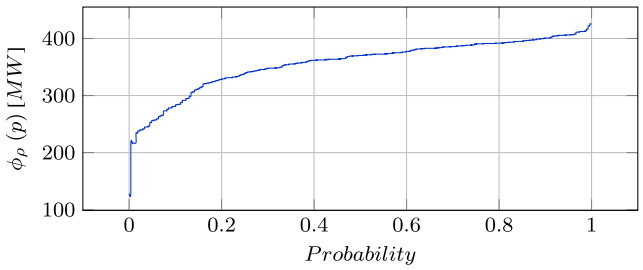

FIGURE 18. Quantile function of solar power at 12 pm (——).

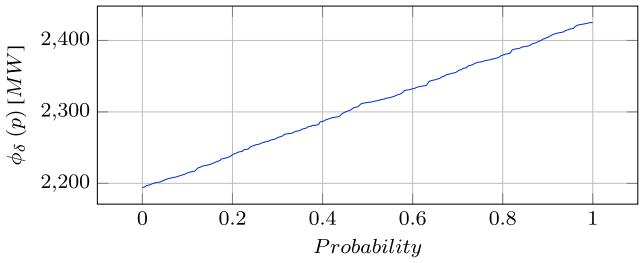

FIGURE 19. Quantile function of load at 12 pm (——).

is considered. This alters the generation of thermal power (Figure 16) which changes the value of the objective function that is directly linked with the value of this variable. Thus, the larger the renewable power is, the lower the thermal power is until the lower limit of the thermal unit and line capacities allow it.

Additionally, Figures 17, 18, and 19 depict the quantile function for wind power, solar power, and power consumed. For the sake of simplicity, these figures were drawn just for an hour since the quantile functions keep the same shape for all hours, except for the function of solar power at hours when there is no solar radiation. In this case, said function is a straight line located in $\phi_\rho = 0$. The reason for this is that the power produced in this period is equal to zero.

Both the quantile functions of solar and wind power (see Figures 17 and 18) show that, if it is required to comply constraint (18) with a higher probability, the value of ϕ_ρ is going to be lower. The reason for this is that, as ζ increases, the value $1-\zeta$ decreases, which produces a movement to the left in both figures. This implies that, in the quantile function, which is always growing, the value of ϕ_ρ decreases when a movement to the left is carried out. Consequently, when

TABLE 4. Minimum operation costs.

Model	Objective function value [CU]	CPU Time [s]
STHS-SOC	925866	4.7
DWS/STHS-SOC	772725	22.7813
RWS/STHS-SOC case I $\zeta = 80\%$	842719	25.6563
RWS/STHS-SOC case II $\zeta = 60\%$	777291	24.1563

$\zeta = 80\%$ both wind, and solar generation are less than when $\zeta = 60\%$ (See Figures 13 and 14).

The behavior of the quantile function of load demand is somewhat different (see Figure 19). In this case, if it is required to increase the probability of holding constraint (20), the value of ϕ_δ increases, which increases the value of load demand when $\zeta = 80\%$ compared with when $\zeta = 60\%$. Figure 15 depicts this behavior.

Consequently, under this approach, the generation of renewable sources is underestimated and the load is overestimated to ensure that the generated power is going to supply the consumed power. This behavior impacts the objective function, as Table 4 shows. The reason for this is that when the renewable source production decreases and the load increases, the thermal unit has to produce more to keep the power balance, as Figure 16 depicts. Thereby, the operation costs are higher.

It addition, it can be seen that, for the DWS/STHS-SOC model and the RWS/STHS-SOC model case II, the values of solar power and power consumed are similar. Likewise, wind power for both cases are comparable, with a gap between 0 and 11 hours. This implies that using mean values of data to carry out the scheduling is an assumption that only allows values around 60% of robustness.

It is important to mention that several simulations (for each model) were carried out to verify the uniqueness of the proposed methodology. All simulations gave the same optimal value, which is one of the main characteristics and advantages of convex optimization compared with metaheuristic techniques, where the convergence point varies each time that the algorithm is run. The costs of the objective function and the CPU times are presented in Table 4.

VI. SUMMARY OF RESULTS

- The proposed SOC approximation for STHS gives an optimum of 925866.00 *CU* with a convergence time of 4.7 S. This value of the objective function is between the range of results of other algorithms that do not consider rigorous mathematics. Comparing these results gives us a good idea of how close the proposed methodology is to the optimum.
- The impact of renewable energy integration in a traditional hydrothermal system is analyzed. Thus, the generation costs reduce 16.5% (DWS/STHS-SOC), 8.9% (RWS/STHS-SOC model case I), and 16% (RWS/STHS-SOC case II), in comparison to results obtained by STHS-SOC.
- The spillage of reservoir 3 tends to be $2 \times 10^4 \frac{m^3}{s}$ as much as possible. This can be explained from two

different perspectives. First, the higher efficiency of unit 4 compared with unit 3 makes the optimization model produce more power with unit 4 instead of unit 3, which promotes spilling water from reservoir 3 to reservoir 4. Second, by analyzing the dual variable of upper spillage, it is observed that these constraints impact the objective function considerably (see Figures 12).

- Since the main values of wind speed and solar irradiation only ensure a robustness close to 60% (Figures 13 and 14), these measures are an inaccurate methodology to predict the power produced by renewable energy.
- As higher robustness is considered, lower renewable generation and higher demand values are obtained, which implies higher production costs.

VII. CONCLUSION

A SOC relaxation was carried out, which showed a superior performance (faster CPU time and lower computational complexity) compared with several techniques studied before, though we have to be careful with a direct comparison as mentioned previously. Besides, under this approach, linearizations are not necessary since it faces the real geometry of the problem, in a mathematically rigorous way, and it is much simpler than the SDP relaxation presented in previous studies.

It was confirmed that convex relaxation gives a global optimum for the approximated Short-Term Hydrothermal Coordination model, something that is not possible to find when heuristic algorithms are used.

The dual variable of the upper limit of spillage was analyzed. It was found that the spillage should not be ignored in this problem, since the study of its dual variable shows that it affects the objective function considerably when hydrochains are considered. It is important to highlight that this kind of analysis cannot be carried out with heuristic and metaheuristic techniques.

A robust model, which considered the stochastic nature of the renewable sources and load demand, was developed by defining upper bounds for the generated power and lower bounds for power demand as chance-box constraints. This methodology turns out to be conservative for wind generation due to the shape of its quantile function, which increases slowly as probability increases. Therefore, a scenarios approach can be more suitable when it comes to wind power. Conversely, the quantile function of solar power increases faster, which results in a not-so-conservative deterministic equivalent for the constraint related to power produced by solar units. Furthermore, the robustness of load demand, under this approach, varies in a linear way in a small interval; this makes sense if the high accuracy of load prediction and its normal distribution are considered.

It was observed that using the mean value of data of the stochastic variables does not represent the real behavior of said variables. This is because, by using this approach, a robustness of only 60% can be guaranteed.

Including the unit commitment and developing a more accurate model that includes the topology, time delays, tailrace, energy storage devices, polynomial hydro power functions, and the interdependence of the stochastic variables will be topics for further research and development.

APPENDIX A
EQUATION DEMONSTRATION

To prove that (8) can be rewritten as:

$$\left\| \begin{pmatrix} \sqrt{c_{1i}}v_{it} - \dfrac{c_{3i}q_{it}}{2\sqrt{c_{1i}}} \\ \sqrt{c_{2i} - \dfrac{c_{3i}^2}{4c_{1i}}}q_{it} \\ \dfrac{1}{2}(1-u_{it}) \end{pmatrix} \right\| \leq \frac{1+u_{it}}{2} \tag{22}$$

Let us consider the following auxiliary variables:

$$k_{it} = \sqrt{c_{1i}}v_{it} - \frac{c_{3i}q_{it}}{2\sqrt{c_{1i}}} \tag{23}$$

$$e_{it} = \sqrt{c_{2i} - \frac{c_{3i}^2}{4c_{1i}}}q_{it} \tag{24}$$

By replacing (23) and (24) in (22) and calculating the Euclidean norm of the vector to the right side, we obtain the following expression:

$$\sqrt{k_{it}^2 + e_{it}^2 + \left(\frac{1-u_{it}}{2}\right)^2} \leq \frac{1+u_{it}}{2} \tag{25}$$

By raising both sides of the previous expression to the second power, we obtain:

$$k_{it}^2 + e_{it}^2 + \left(\frac{1-u_{it}}{2}\right)^2 \leq \left(\frac{1+u_{it}}{2}\right)^2 \tag{26}$$

Note that $k_{it}^2+e_{it}^2 = c_{1i}v_{it}^2+c_{2i}q_{it}^2-c_{3i}q_{it}v_{it}$ and $\left(\frac{1-u_{it}}{2}\right)^2 - \left(\frac{1+u_{it}}{2}\right)^2 = -u_{it}$. Therefore, (26) can be rewritten as:

$$c_{1i}v_{it}^2 + c_{2i}q_{it}^2 - c_{3i}q_{it}v_{it} - u_{it} \leq 0 \tag{27}$$

Recovering the value of the auxiliary variable $u_{it} = c_{4i}v_{it} + c_{5i}q_{it} + c_{6i} - p_{it}^{\mathsf{h}}$ and organizing our expression, we finally obtain (28), which proves that a quadratic constraint can be rewritten as a Second-Order Cone constraint.

$$p_{it}^{\mathsf{h}} \leq -c_{1i}v_{it}^2 - c_{2i}q_{it}^2 + c_{3i}q_{it}v_{it} + c_{4i}v_{it} + c_{5i}q_{it} + c_{6i} \tag{28}$$

APPENDIX B
LINEARIZATION OF THE PROBLEM

To analyze the loss of information when linearizations are carried out for the STHTS problem, the MATLAB curve fitting tool was used to carry out linear approximations of the hydropower equations. Thus, said equations take the following structure:

$$pl_{it}^{\mathsf{h}} = c_{l_{1_i}}v_{it} + c_{l_{2_i}}q_{it} + c_{l_{3_i}} \tag{29}$$

TABLE 5. Hydropower coefficients linearization.

Plant	$c_{l_{1_i}}$	$c_{l_{2_i}}$	$c_{l_{3_i}}$
1	0.5775	4.55	-21.97
2	0.234	5.05	7.755
3	0.286	-4.12	65.92
4	1.263	5.325	-3.222

where the coefficient of the linearization are given in Table 5.

It is worth mentioning that the linearizations were carried out for the intervals between $q_{min} - q_{max}$ and $v_{min} - v_{max}$, which were taken from [20]. Said linearization was a polynomial one.

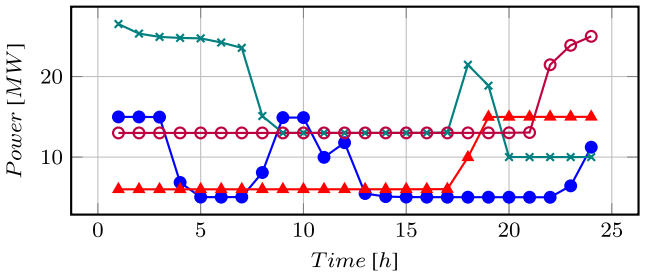

FIGURE 20. Water discharge of hydro units (linearized model).

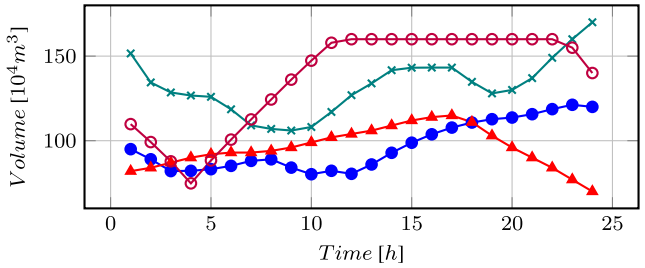

FIGURE 21. Volumes of reservoirs (Linearized model).

Figures 20 and 21 present the water discharges and the volumes of reservoirs obtained when (29) is considered. These values were replaced in both (2) and (29), obtaining the power produced for all units in both cases (Tables 6 and 7). In doing so, the results show a considerable difference between the power produced with the non-convex equation and the linear equation, when the values of Figures 20 and 21 are considered (Table 8).

Note that the hydropower difference between the linear equations and the results of the quadratic equation are close to 20 *MW* (Table 8) in most time intervals, which sums to a total difference in a day of 536.87 *MW*. This gap is considerable if we take into account the size of the test system, and it gives us an idea about how much information can be lost when linearizations are carried out. In addition, the values of volumes and water discharges for unit 3 in the first 5 hours, provided by the linearized model, gives negative values when they are replaced in the quadratic equation that models the real behavior of this unit (see Table 7). This implies that the linearized model is giving non-feasible operation points since these negative values would mean that unit 3 is working as a pump that consumes power.

TABLE 6. Power produced by hydro units using linearized equations [MW].

Hour	pl_1^h	pl_2^h	pl_3^h	pl_4^h
1	105.6932	52.6906	0.0062	204.6809
2	104.2675	53.8450	0.0069	191.2934
3	102.5468	55.5769	0.0078	176.8956
4	61.5994	57.3089	0.0092	160.4768
5	52.6454	58.4635	0.0114	177.5541
6	53.0680	59.0409	0.0162	193.1292
7	53.8579	59.0410	0.0309	208.1842
8	69.4197	59.6189	34.2951	223.0804
9	102.7140	60.7744	42.6685	237.9085
10	101.7906	62.5072	43.2688	252.0888
11	77.3563	64.2397	45.8071	265.4297
12	86.1090	65.3960	48.6439	268.0867
13	55.5356	66.5521	50.6290	268.0880
14	55.2227	68.2870	52.8507	268.0888
15	56.3398	70.0235	53.2542	268.0925
16	57.4286	71.1879	53.2365	268.0941
17	58.3534	71.8122	53.1094	268.1005
18	59.0370	87.4615	16.0472	268.1090
19	59.5018	105.6468	24.7828	268.1303
20	59.7152	101.6503	61.8656	268.1823
21	60.1614	98.2153	63.8951	268.3506
22	60.8363	94.7695	67.3256	313.1363
23	68.6142	90.7320	70.4712	319.6652
24	92.5393	86.6933	73.3307	306.6811

TABLE 7. Power produced by hydro units using quadratic equations [MW].

Hour	pq_1^h	pq_2^h	pq_3^h	pq_4^h
1	95.8476	50.1732	-2.2545	200.0943
2	92.3943	51.3047	-0.4761	187.7564
3	87.9989	52.9424	-0.1429	173.7349
4	61.3087	54.5082	-0.0684	156.7936
5	48.0690	55.5122	-0.0376	174.3935
6	48.6838	56.0028	0.1007	189.4890
7	49.8031	56.0037	-0.0403	203.2134
8	71.8260	56.4874	37.7835	215.9544
9	89.3310	57.4297	40.4192	227.8087
10	86.7649	58.7822	41.2324	238.3724
11	78.1599	60.0626	44.5423	247.6220
12	83.1812	60.8794	47.9279	249.3908
13	52.6362	61.6647	50.1211	249.3925
14	51.6135	62.7837	52.3878	249.3950
15	52.6128	63.8349	52.7934	249.4008
16	53.4774	64.5114	52.8127	249.4048
17	54.1132	64.9213	52.8022	249.4165
18	54.4862	88.7248	25.4222	249.4330
19	54.7124	103.0983	34.9574	249.4735
20	54.7815	99.1402	47.6731	249.5728
21	54.9221	95.4299	49.5010	249.8970
22	55.0753	91.4254	52.2900	313.9870
23	67.7341	86.3820	54.4429	318.5734
24	97.2746	80.9460	56.0642	303.5320

TABLE 8. Total hydropower using linearized equations, total hydropower using quadratic equations and difference between the total hydropower using linearized equations and the total hydropower using quadratic equations (HPDLQ) [MW].

Hour	Tpl^h	Tpq^h	$HPDLQ$
1	363.0708	343.8607	19.2101
2	349.4127	330.9794	18.4334
3	335.0271	314.5332	20.4939
4	279.3943	272.5422	6.8521
5	288.6744	277.9371	10.7373
6	305.2543	294.2763	10.9780
7	321.1140	308.9799	12.1341
8	386.4140	382.0512	4.3628
9	444.0653	414.9886	29.0767
10	459.6554	425.1520	34.5034
11	452.8328	430.3867	22.4461
12	468.2356	441.3793	26.8563
13	440.8046	413.8145	26.9901
14	444.4492	416.1800	28.2691
15	447.7101	418.6420	29.0681
16	449.9471	420.2062	29.7409
17	451.3755	421.2532	30.1223
18	430.6547	418.0661	12.5886
19	458.0617	442.2417	15.8200
20	491.4135	451.1677	40.2458
21	490.6224	449.7501	40.8723
22	536.0677	512.7777	23.2900
23	549.4827	527.1324	22.3503
24	559.2444	537.8169	21.4275

REFERENCES

[1] S. Ruzic, A. Vuckovic, and N. Rajakovic, "A flexible approach to short-term hydro-thermal coordination. II. Dual problem solution procedure," *IEEE Trans. Power Syst.*, vol. 11, no. 3, pp. 1572–1578, Aug. 1996.

[2] S. Ruzic and R. Rajakovic, "Optimal distance method for Lagrangian multipliers updating in short-term hydro-thermal coordination," *IEEE Trans. Power Syst.*, vol. 13, no. 4, pp. 1439–1444, Nov. 1998.

[3] H. Habibollahzadeh and J. A. Bubenko, "Application of decomposition techniques to short-term operation planning of hydrothermal power system," *IEEE Trans. Power Syst.*, vol. PWRS-1, no. 1, pp. 41–47, Feb. 1986.

[4] C.-A. Li, P. J. Jap, and D. L. Streiffert, "Implementation of network flow programming to the hydrothermal coordination in an energy management system," *IEEE Trans. Power Syst.*, vol. 8, no. 3, pp. 1045–1053, Aug. 1993.
[5] X. Qing, X. Niande, W. Shiying, Z. Boming, and H. Mei, "Optimal daily scheduling of cascaded plants using a new algorithm of nonlinear minimum cost network flow," *IEEE Trans. Power Syst.*, vol. PWRS-3, no. 3, pp. 929–935, Aug. 1988.
[6] N. J. Redondo and A. J. Conejo, "Short-term hydro-thermal coordination by Lagrangian relaxation: Solution of the dual problem," *IEEE Trans. Power Syst.*, vol. 14, no. 1, pp. 89–95, Feb. 1999.
[7] N. Petcharaks and W. Ongsakul, "Hybrid enhanced lagrangian relaxation and quadratic programming for hydrothermal scheduling," *Electr. Power Compon. Syst.*, vol. 35, no. 1, pp. 19–42, Feb. 2007.
[8] M. S. Salam, K. M. Nor, and A. R. Hamdan, "Comprehensive algorithm for hydrothermal coordination," *IEE Proc.—Gener., Transmiss. Distrib.*, vol. 144, no. 5, pp. 482–488, Sep. 1997.
[9] Q. Goor, R. Kelman, and A. Tilmant, "Optimal multipurpose-multireservoir operation model with variable productivity of hydropower plants," *J. Water Resour. Planning Manage.*, vol. 137, no. 3, pp. 258–267, May 2011.
[10] J. Tang and P. B. Luh, "Hydrothermal scheduling via extended differential dynamic programming and mixed coordination," *IEEE Trans. Power Syst.*, vol. 10, no. 4, pp. 2021–2028, Nov. 1995.
[11] A. L. Diniz and M. E. P. Maceira, "A four-dimensional model of hydro generation for the short-term hydrothermal dispatch problem considering head and spillage effects," *IEEE Trans. Power Syst.*, vol. 23, no. 3, pp. 1298–1308, Aug. 2008.
[12] J. Jian, S. Pan, and L. Yang, "Solution for short-term hydrothermal scheduling with a logarithmic size mixed-integer linear programming formulation," *Energy*, vol. 171, pp. 770–784, Mar. 2019.
[13] E. Parrilla and J. García-González, "Improving the B&B search for large-scale hydrothermal weekly scheduling problems," *Int. J. Electr. Power Energy Syst.*, vol. 28, no. 5, pp. 339–348, Jun. 2006.
[14] G. W. Chang, M. Aganagic, J. G. Waight, J. Medina, T. Burton, S. Reeves, and M. Christoforidis, "Experiences with mixed integer linear programming based approaches on short-term hydro scheduling," *IEEE Trans. Power Syst.*, vol. 16, no. 4, pp. 743–749, Nov. 2001.
[15] O. Nilsson and D. Sjelvgren, "Mixed-integer programming applied to short-term planning of a hydro-thermal system," *IEEE Trans. Power Syst.*, vol. 11, no. 1, pp. 281–286, Feb. 1996.
[16] Y. Lu, J. Zhou, H. Qin, Y. Wang, and Y. Zhang, "An adaptive chaotic differential evolution for the short-term hydrothermal generation scheduling problem," *Energy Convers. Manage.*, vol. 51, no. 7, pp. 1481–1490, Jul. 2010.
[17] A. Haghrah, B. Mohammadi-Ivatloo, and S. Seyedmonir, "Real coded genetic algorithm approach with random transfer vectors-based mutation for short-term hydro–thermal scheduling," *IET Gener., Transmiss. Distrib.*, vol. 9, no. 1, pp. 75–89, Jan. 2015.
[18] J. S. Dhillon, J. S. Dhillon, and D. P. Kothari, "Real coded genetic algorithm for stochastic hydrothermal generation scheduling," *J. Syst. Sci. Syst. Eng.*, vol. 20, no. 1, pp. 87–109, Mar. 2011.
[19] Y. Wang, J. Zhou, L. Mo, R. Zhang, and Y. Zhang, "Short-term hydrothermal generation scheduling using differential real-coded quantum-inspired evolutionary algorithm," *Energy*, vol. 44, no. 1, pp. 657–671, Aug. 2012.
[20] S. O. Orero and M. R. Irving, "A genetic algorithm modelling framework and solution technique for short term optimal hydrothermal scheduling," *IEEE Trans. Power Syst.*, vol. 13, no. 2, pp. 501–518, May 1998.
[21] J. Zhang, J. Wang, and C. Yue, "Small population-based particle swarm optimization for short-term hydrothermal scheduling," *IEEE Trans. Power Syst.*, vol. 27, no. 1, pp. 142–152, Feb. 2012.
[22] Y. Wu, Y. Wu, and X. Liu, "Couple-based particle swarm optimization for short-term hydrothermal scheduling," *Appl. Soft Comput.*, vol. 74, pp. 440–450, Jan. 2019.
[23] A. Rasoulzadeh-Akhijahani and B. Mohammadi-Ivatloo, "Short-term hydrothermal generation scheduling by a modified dynamic neighborhood learning based particle swarm optimization," *Int. J. Electr. Power Energy Syst.*, vol. 67, pp. 350–367, May 2015.
[24] R. K. Swain, A. K. Barisal, P. K. Hota, and R. Chakrabarti, "Short-term hydrothermal scheduling using clonal selection algorithm," *Int. J. Electr. Power Energy Syst.*, vol. 33, no. 3, pp. 647–656, Mar. 2011.
[25] H. M. Dubey, M. Pandit, and B. K. Panigrahi, "Ant lion optimization for short-term wind integrated hydrothermal power generation scheduling," *Int. J. Electr. Power Energy Syst.*, vol. 83, pp. 158–174, Dec. 2016.
[26] T. T. Nguyen and D. N. Vo, "Modified cuckoo search algorithm for multiobjective short-term hydrothermal scheduling," *Swarm Evol. Comput.*, vol. 37, pp. 73–89, Dec. 2017.
[27] K. Sörensen, "Metaheuristics—The metaphor exposed," *Int. Trans. Oper. Res.*, vol. 22, no. 1, pp. 3–18, Jan. 2015.
[28] R. Fuentes-Loyola and V. H. Quintana, "Medium-term hydrothermal coordination by semidefinite programming," *IEEE Trans. Power Syst.*, vol. 18, no. 4, pp. 1515–1522, Nov. 2003.
[29] Y. Zhu, J. Jian, J. Wu, and L. Yang, "Global optimization of non-convex hydro-thermal coordination based on semidefinite programming," *IEEE Trans. Power Syst.*, vol. 28, no. 4, pp. 3720–3728, Nov. 2013.
[30] J. Zhou, P. Lu, Y. Li, C. Wang, L. Yuan, and L. Mo, "Short-term hydro-thermal-wind complementary scheduling considering uncertainty of wind power using an enhanced multi-objective bee colony optimization algorithm," *Energy Convers. Manage.*, vol. 123, pp. 116–129, Sep. 2016.
[31] C. Li, W. Wang, and D. Chen, "Multi-objective complementary scheduling of hydro-thermal-RE power system via a multi-objective hybrid grey wolf optimizer," *Energy*, vol. 171, pp. 241–255, Mar. 2019.
[32] S. Das, A. Bhattacharya, and A. K. Chakraborty, "Fixed head short-term hydrothermal scheduling in presence of solar and wind power," *Energy Strategy Rev.*, vol. 22, pp. 47–60, Nov. 2018.
[33] B. P. Cotia, C. L. T. Borges, and A. L. Diniz, "Optimization of wind power generation to minimize operation costs in the daily scheduling of hydrothermal systems," *Int. J. Electr. Power Energy Syst.*, vol. 113, pp. 539–548, Dec. 2019.
[34] W. van Ackooij, E. C. Finardi, and G. M. Ramalho, "An exact solution method for the hydrothermal unit commitment under wind power uncertainty with joint probability constraints," *IEEE Trans. Power Syst.*, vol. 33, no. 6, pp. 6487–6500, Nov. 2018.
[35] J. Wang, M. Guo, and Y. Liu, "Hydropower unit commitment with nonlinearity decoupled from mixed integer nonlinear problem," *Energy*, vol. 150, pp. 839–846, May 2018.
[36] G. E. Alvarez, M. G. Marcovecchio, and P. A. Aguirre, "Security-constrained unit commitment problem including thermal and pumped storage units: An MILP formulation by the application of linear approximations techniques," *Electr. Power Syst. Res.*, vol. 154, pp. 67–74, Jan. 2018.
[37] J. Zhang, Q. Tang, Y. Chen, and S. Lin, "A hybrid particle swarm optimization with small population size to solve the optimal short-term hydro-thermal unit commitment problem," *Energy*, vol. 109, pp. 765–780, Aug. 2016.
[38] W. Wang, C. Li, X. Liao, and H. Qin, "Study on unit commitment problem considering pumped storage and renewable energy via a novel binary artificial sheep algorithm," *Appl. Energy*, vol. 187, pp. 612–626, Feb. 2017.
[39] R. S. Patwal, N. Narang, and H. Garg, "A novel TVAC-PSO based mutation strategies algorithm for generation scheduling of pumped storage hydrothermal system incorporating solar units," *Energy*, vol. 142, pp. 822–837, Jan. 2018.
[40] M. S. Salam, *Handbook of Power Systems I*. Berlin, Germany: Springer, 2010.
[41] N. Amjady and M. Reza Ansari, "Hydrothermal unit commitment with AC constraints by a new solution method based on benders decomposition," *Energy Convers. Manage.*, vol. 65, pp. 57–65, Jan. 2013.
[42] A. Abdolahi, F. S. G. A. Alizadeh, and A. T. Kalantari, "Chance-constrained caes and drp scheduling to maximize wind power harvesting in congested transmission systems considering operational flexibility," *Sustain. Cities Soc.*, vol. 51, pp. 1–12, Nov. 2019.
[43] M. Belsnes, J. Roynstrand, and B. O. Fosso, "Handling state dependent nonlinear tunnel flows in short-term hydropower scheduling," in *Proc. Int. Conf. Power Syst. Technol.*, Nov. 2004, pp. 1410–1415.
[44] J. Kong, H. I. Skjelbred, and O. B. Fosso, "An overview on formulations and optimization methods for the unit-based short-term hydro scheduling problem," *Electr. Power Syst. Res.*, vol. 178, pp. 1–14, Jan. 2020.
[45] H. I. Skjelbred, J. Kong, and O. B. Fosso, "Dynamic incorporation of nonlinearity into MILP formulation for short-term hydro scheduling," *Int. J. Elect. Power Energy Syst.*, vol. 116, pp. 1–17, Mar. 2020.
[46] L. S. M. Guedes, P. de Mendonca Maia, A. C. Lisboa, D. A. G. Vieira, and R. R. Saldanha, "A unit commitment algorithm and a compact MILP model for short-term hydro-power generation scheduling," *IEEE Trans. Power Syst.*, vol. 32, no. 5, pp. 3381–3390, Sep. 2017.
[47] T.-B. Deng, "Minimax design of low-complexity even-order variable fractional-delay filters using second-order cone programming," *IEEE Trans. Circuits Syst. II, Exp. Briefs*, vol. 58, no. 10, pp. 692–696, Oct. 2011.

[48] J. Liu, A. B. Gershman, Z.-Q. Luo, and K. M. Wong, "Adaptive beamforming with sidelobe control," *IEEE Signal Process. Lett.*, vol. 10, no. 11, pp. 331–334, Nov. 2003.
[49] Y. Zhou, Y. Tian, K. Wang, and M. Ghandhari, "Robust optimisation for AC DC power flow based on second order cone programming," *J. Eng.*, vol. 2017, Oct. 2017, Art. no. 21642167.
[50] F. Alizadeh and D. Goldfarb, "Second-order cone programming," *Math. Program.*, vol. 95, no. 1, pp. 3–51, Jan. 2003.
[51] T. M. Goodrich, R. Tamassia, and H. M. Goldwasser, *Data Structures and Algorithms*. Hoboken, NJ, USA: Wiley, 2014.
[52] N. Karmarkar, "A new polynomial-time algorithm for linear programming," *Combinatorica*, vol. 4, no. 4, pp. 373–395, Dec. 1984.
[53] T. S. Rao, S. S. Rao, and C. R. Rao, *Handbook of Statistics*. Amsterdam, The Netherlands: Elsevier, 2012.
[54] S. Vedula and P. P. Mujumdar, *Water Resources Systems: Modelling and Techniques and Analysis*. New York, NY, USA: McGraw-Hill, 2007.
[55] J. Machowski, W. J. Bialek, and R. J. Bumby, *Power System Dynamics: Stability and Control*. Hoboken, NJ, USA: Wiley, 2008.
[56] P. Kundur, *Power System Stability and Control*. New York, NY, USA: McGraw-Hill, 1994.
[57] M. Victoria and B. G. Andresen, "Using validated reanalysis data to investigate the impact of the PV system configurations at high penetration levels in European countries," *Prog. Photovolt., Res. Appl.*, vol. 27, no. 7, pp. 576–592, 2019.
[58] K. R. Padiyar, *Power System Dynamics and Stability and Control*. New Delhi, India: BS Publications, 2008.
[59] S. Das, A. Bhattacharya, and A. K. Chakraborty, "Solution of short-term hydrothermal scheduling problem using quasi-reflected symbiotic organisms search algorithm considering multi-fuel cost characteristics of thermal generator," *Arabian J. Sci. Eng.*, vol. 43, no. 6, pp. 2931–2960, Jun. 2018.
[60] P. S. Oliveto, J. He, and X. Yao, "Time complexity of evolutionary algorithms for combinatorial optimization: A decade of results," *Int. J. Autom. Comput.*, vol. 4, no. 3, pp. 281–293, Jul. 2007.
[61] J. He and X. Yao, "Drift analysis and average time complexity of evolutionary algorithms," *Artif. Intell.*, vol. 127, pp. 28–57, Mar. 2001.
[62] D. Sudholt and C. Witt, "Runtime analysis of a binary particle swarm optimizer," *Theor. Comput. Sci.*, vol. 411, no. 21, pp. 2084–2100, May 2010.

JUAN CAMILO CASTAÑO (Member, IEEE) was born in Pereira, Colombia, in 1990. He received the bachelor's degree in electrical engineering and the master's degree in power systems engineering from the Universidad Tecnológica de Pereira, Pereira, in 2015 and 2020, respectively. From 2015 to 2017, he was a distribution grid design engineer with several Colombian companies. Since 2018, he has been an Adjunct Professor with the Department of Electric Power Engineering, Universidad Tecnológica de Pereira. His current research interests include hydrothermal coordination, renewable energies, mathematical optimization, and optimization in distribution grids.

ALEJANDRO GARCES (Senior Member, IEEE) was born in Pereira, Colombia, in 1981. He received the bachelor's degree in electrical engineering and the master's degree in power systems engineering from the Universidad Tecnológica de Pereira, Pereira, in 2004 and 2006, respectively, and the Ph.D. degree from the Norwegian University of Science and Technology (NTNU), Trondheim, Norway, in 2012. He was a Research Fellow with NTNU. He was also a Consultant with the Inter-American Development Bank, the Latin-American Organization of Energy, and the Energy and Gas Regulation Commission, Colombia. He has participated in the study Smart Grids Colombia Vision 2030, that defined the roadmap for the implementation of smart grids in Colombia. He is currently an Assistant Professor with the Department of Electric Power Engineering, Universidad Tecnológica de Pereira. His current research interests include mathematical optimization and control for power systems applications, dynamics in electric grids, renewable energies, energy storage devices, microgrids, and HVDC transmission.

OLAV B. FOSSO (Senior Member, IEEE) is currently a Professor with the Department of Electric Power Engineering, Norwegian University of Science and Technology (NTNU). Previously, he was a Scientific Advisor and a Senior Research Scientist with the SINTEF Energy Research, the Head of the Department of Electric Power Engineering, from 2009 to 2013, and the Director of the NTNUs Strategic Thematic Area Energy, from September 2014 to September 2016. He is currently the Deputy Head of the Department of Electric Power Engineering with responsibility for research. His research interests include hydro scheduling, market integration of intermittent generation, and signal analysis for study of power system's dynamics and stability. He was the Chairman of the CIGRE SC C5 Electricity Markets and Regulation; a member of the CIGRE Technical Committee, from 2008 to 2014; the Chairman of the Board of Norwegian Research Centre for Offshore Wind Technology (NOWITECH), from 2015 to 2017; and a Board Member of the Energy21 (Norwegian National Strategy for Research, Development, Demonstration and Commercialization of New Energy Technology), from 2015 to 2018. He has been an Expert Evaluator with the Horizon 2020 and a number of science foundations internationally.